# Device operation of conjugated polymer/zinc oxide bulk heterojunction solar cells

Koster, Lambert; van Strien, Wouter J.; Beek, Waldo J. E.; Blom, Paul W. M.

*Published in:*
Advanced Functional Materials

*DOI:*
10.1002/adfm.200600371



*Publication date:*
2007

ADVANCED FUNCTIONAL MATERIALS

FULL PAPER

DOI: 10.1002/adfm.200600371

# Device Operation of Conjugated Polymer/Zinc Oxide Bulk Heterojunction Solar Cells**

By *L. Jan Anton Koster*, *Wouter J. van Strien*, *Waldo J. E. Beek*, and *Paul W. M. Blom**

Solar cells based on a poly(*p*-phenylene vinylene) (PPV) derivative and zinc oxide nanoparticles can reach a power conversion efficiency of 1.6 %. The transport of electrons and holes in these promising devices is characterized and it is found that the electron mobility is equal to $2.8 \times 10^{-9}$ $m^2 V^{-1} s^{-1}$, whereas the hole mobility amounts to $5.5 \times 10^{-10}$ $m^2 V^{-1} s^{-1}$. By modeling the current–voltage characteristics under illumination it is found that the performance of PPV/zinc oxide solar cells is limited by the charge-carrier mobilities. Subsequently, how to further improve the efficiency is discussed.

## 1. Introduction

The advantages of solution processing, for example, the potential to fabricate low-cost large area devices, make solar cells based on conjugated polymers very attractive. One major difference between polymer-based solar cells and inorganic solar cells is that upon light absorption by the polymer, an exciton is created. The exciton binding energy typically amounts to 0.4 eV,[1] making exciton dissociation in a pristine conjugated polymer very inefficient. By mixing in an electron acceptor, a substance with a higher electron affinity than the polymer, it is possible to break up the exciton by transferring the electron from the polymer onto the electron acceptor.[2] So far, several electron acceptors have been shown to yield efficient devices: conjugated polymers,[3] fullerenes,[4] and inorganic nanocrystals.[5] In the class of inorganic acceptors, metal oxides are among the most studied materials. $TiO_2$ has been studied in several forms: nanoparticles,[6,7] porous networks,[8] and in situ formation of $TiO_2$ from a precursor.[9] Recently, zinc oxide nanoparticles (nc-ZnO) have also been used as an electron-accepting material, in combination with poly(2-methoxy-5-(3′,7′-dimethyloctyloxy)-*p*-phenylene vinylene) (MDMO-PPV), with an AM1.5 (AM: air mass) efficiency of 1.6 %.[10] ZnO has several merits: ZnO is a cheap and environmentally friendly material that can be produced in crystalline form at low temperature. Furthermore, it displays good transport properties, even in films consisting of nanoparticles.[11]

Although MDMO-PPV/nc-ZnO solar cells are certainly promising, the efficiency is lower than that of the related MDMO-PPV/$C_{61}$-butyric acid methyl ester (PCBM) system, which has an efficiency of 2.5 %.[12] The question arises: what causes the lower efficiency of MDMO-PPV/nc-ZnO solar cells and how, if possible, might this be resolved? In this article, we study the transport properties of blends of MDMO-PPV and nc-ZnO, model the current–voltage characteristics, identify the factors limiting the performance, and discuss whether these limitations can be removed.

## 2. Results and Discussion

ZnO nanoparticles of approximately 5 nm in diameter were synthesized by hydrolyzing and condensing zinc acetate dihydrate by using KOH in methanol, using the method of Pacholski et al.[10,13] Photovoltaic devices consisted of an active layer of nc-ZnO and MDMO-PPV spin-cast from a mixture of methanol and chlorobenzene. This blend is sandwiched between a transparent layer of indium tin oxide (ITO) coated by a hole-conducting layer of poly(3,4-ethylenedioxythiophene)/poly(styrene sulfonate) (PEDOT:PSS), typically of 60 nm thickness, and an evaporated LiF (1 nm)/Al (100 nm) top electrode. The optimum mass ratio for the MDMO-PPV/nc-ZnO device is 1:2, corresponding to 25 vol % ZnO.[10]

So-called hole-only devices (electron injection suppressed) were obtained by spin-casting the active layer directly onto ITO, while the LiF/Al cathode was replaced by an evaporated Au electrode. In order to fabricate electron-only diodes, a 1 nm Cr layer was evaporated on glass substrates, followed by

[*] Prof. P. W. M. Blom, W. J. van Strien
Materials Science Centre$^{Plus}$
University of Groningen
Nijenborgh 4, 9747 AG Groningen (The Netherlands)
E-mail: p.w.m.blom@rug.nl
Dr. L. J. A. Koster
Materials Science Centre$^{Plus}$ and Dutch Polymer Institute
University of Groningen
Nijenborgh 4, 9747 AG Groningen (The Netherlands)
Dr. W. J. E. Beek
Laboratory of Macromolecular and Organic Chemistry
Eindhoven University of Technology
P.O. Box 513, 5600 MB Eindhoven (The Netherlands)

[**] The authors are indebted to J. Sweelssen (TNO Science and Industry) for a generous supply of MDMO-PPV. Furthermore, Dr. M. M. Wienk and Prof. Dr. R. A. J. Janssen are acknowledged for useful discussions. One of the authors (L.J.A.K.) wishes to thank J. Wildeman for technical assistance. The work of this author forms part of the research program of the Dutch Polymer Institute (No. 323).

50 nm of Ag and 10 nm of Sm and the active layer. As a top electrode, 10 nm of Sm topped with 80 nm of Al was employed. Spin-casting on Sm requires some care, as it is a reactive metal, but extensive testing showed no significant degradation of the bottom electrode. However, in this configuration the Sm bottom electrode is not used to inject electrons into the active layer, but only to suppress the injection of holes, while the top electrode supplies the electrons. Solar cells with a MDMO-PPV/nc-ZnO or poly(3-hexylthiophene) (P3HT)/PCBM blend with Sm as a top contact (instead of LiF (1 nm)/Al) show a good performance and, most importantly, an open-circuit voltage equal to devices with LiF/Al as top electrode. Therefore, we can conclude that this makes a good electron-injecting contact.

After fabrication, the current–voltage characteristics of these devices were measured in a N atmosphere both in the dark and under illumination. A white-light halogen lamp was used to illuminate the photovoltaic devices. The UV part of the lamp spectrum was cut with a filter that blocked wavelengths smaller than 435 nm for all measurements under illumination, because the devices degrade very fast when exposed to UV light.[14] The resulting intensity amounts to approximately 720 W m$^{-2}$.

### 2.1. MDMO-PPV/nc-ZnO Solar Cells

Figure 1 shows the current density–voltage characteristics of an MDMO-PPV/nc-ZnO solar cell under illumination. Typically, the open-circuit voltage ranges from 0.7 V to 0.8 V. An approximate schematic of the highest occupied molecular orbital (HOMO) and the lowest unoccupied molecular orbital (LUMO) of MDMO-PPV, and the valence and conduction band of nc-ZnO is shown in the inset of Figure 1. As the conduction band of nc-ZnO (4.2 eV) lies deeper than the LUMO of PCBM (approximately 3.9 eV),[15] it is easy to understand that the open-circuit voltage ($V_{oc}$) of MDMO-PPV/nc-ZnO solar cells is slightly lower when compared to MDMO-PPV/PCBM devices ($V_{oc}$ = 0.80–0.85 V).[12,15] As the effective masses of electrons and holes in ZnO is relatively low, quantum confinement effects already start to play a role at relatively large particle size.[16] Moreover, considerable influence of surface conditions is expected, rendering the exact positions of the electronic levels of nc-ZnO quite sensitive to the circumstances during synthesis.

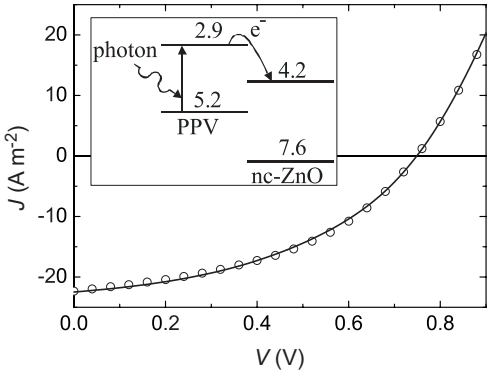


**Figure 1.** Current density–voltage characteristics of an illuminated MDMO-PPV/nc-ZnO solar cell with an active layer thickness of 130 nm (symbols), the line denotes the numerical modeling result. The inset shows the energy levels of the MDMO-PPV/nc-ZnO system.

Figure 2 shows the short-circuit current density $J_{sc}$ as a function of light intensity $I$ of an MDMO-PPV/nc-ZnO solar cell. When fitted to $J_{sc} \propto I^{\alpha}$, $\alpha = 1.03 \pm 0.02$ is obtained, showing that the short-circuit current density is linear in intensity.

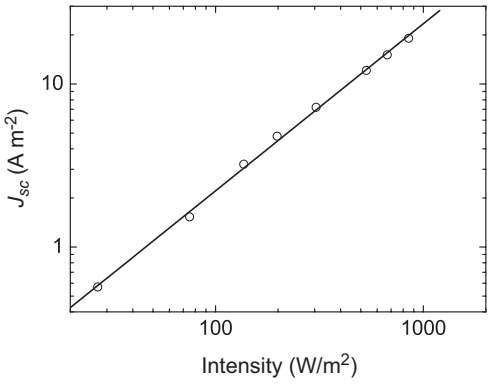


**Figure 2.** The incident-light-intensity dependence on the short-circuit current density of an MDMO-PPV/nc-ZnO photovoltaic device (symbols) and a fit to the relation $J_{sc} \propto I^{\alpha}$, where $\alpha = 1.03 \pm 0.02$ (line).

### 2.2. Charge Transport in MDMO-PPV/nc-ZnO Blends

In order to assess to the transport of holes in MDMO-PPV/nc-ZnO solar cells, the cathode was replaced by a high-work-function electrode, thereby blocking the injection of electrons from the contact. Because the anode could readily supply a very large number of holes, the flow of current through the device was limited by the buildup of space charge. The observation of this so-called space-charge-limited current enables one to obtain the hole mobility directly from the measurements. In the case of a field-dependent mobility of Poole–Frenkel-like form

$$\mu = \mu_0 e^{\gamma\sqrt{V_{int}/L}} \tag{1}$$

where $\mu_0$ is the zero-field mobility, $\gamma$ is the field activation parameter, and $L$ denotes the active layer thickness, one has[17]

$$J_{SC} = \frac{9}{8}\varepsilon\mu_0 e^{0.891\gamma\sqrt{V_{int}/L}}\frac{V_{int}^2}{L^3} \tag{2}$$

where $\varepsilon$ is the dielectric constant. The internal voltage dropped across the active layer, $V_{int}$, is equal to

$$V_{int} = V - V_{bi} - V_{Rs} \tag{3}$$

where $V_{bi}$ is the built-in voltage that arises from the difference in work function between the bottom and top electrode. Because our ITO substrates have a nonnegligible series resistance (typically 30 Ω), the internal voltage has to be corrected for

ADVANCED FUNCTIONAL MATERIALS



the voltage drop $V_{Rs}$ across the substrate. The built-in voltage is determined from the current–voltage characteristics as the voltage at which the current–voltage characteristic becomes quadratic, corresponding to the flat-band voltage. The relative dielectric constant $\varepsilon_r$ for MDMO-PPV is taken as 2.1,[18] whereas $\varepsilon_r = 8.5$ is used for nc-ZnO.[16]

Figure 3 shows current density–voltage characteristics of a pristine MDMO-PPV hole-only diode with an active layer of 90 nm thickness. By fitting the experimental data to Equation 2 and using $V_{bi} = 0.4$ V, a value of $4.0 \times 10^{-10}$ m$^2$ V$^{-1}$ s$^{-1}$ is

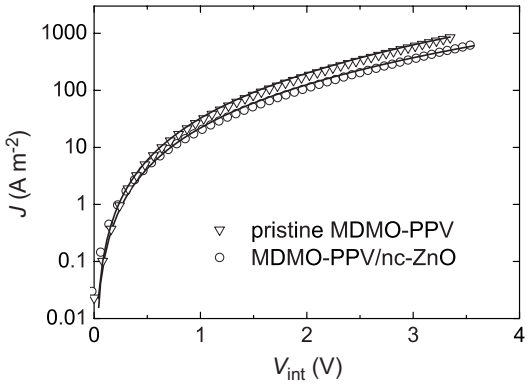


**Figure 3.** Current density–voltage characteristics of hole-only diodes of pristine MDMO-PPV (active layer thickness 90 nm) and MDMO-PPV/nc-ZnO (active layer thickness 130 nm). The lines denote fits to Equation 2.

obtained for the zero-field mobility, together with $\gamma = 3.5 \times 10^{-4}$ (m V$^{-1}$)$^{0.5}$. Note that this batch of MDMO-PPV, synthesized via the sulfinyl route, has a ten times higher hole mobility than previously reported for MDMO-PPV.[19] Figure 3 also shows current density–voltage measurements of an MDMO-PPV/nc-ZnO hole-only diode, with an active layer thickness of 130 nm. Although the blend layer is somewhat thicker than the layer of MDMO-PPV discussed previously, the current densities are very similar. In fact, using $V_{bi} = 0.3$ V a zero-field mobility of $5.5 \times 10^{-10}$ m$^2$ V$^{-1}$ s$^{-1}$ is obtained and $\gamma = 3.5 \times 10^{-4}$ (m V$^{-1}$)$^{0.5}$, showing that, within experimental error, the hole mobility in the polymer phase of the blend is not affected by the presence of nc-ZnO.

The current density–voltage characteristics of an electron-only device with a 115 nm thick active layer consisting of the MDMO-PPV/nc-ZnO blend is depicted in Figure 4. No built-in voltage is subtracted, because the bottom and top electrode consist of the same metal (Sm). Using Equation 2, we find $\mu_0 = 2.8 \times 10^{-9}$ m$^2$ V$^{-1}$ s$^{-1}$ and $\gamma = 0.5 \times 10^{-4}$ (m V$^{-1}$)$^{0.5}$, so the electron mobility is a factor of 5 higher than the hole mobility of the polymer phase. Transport of electrons in nc-ZnO films has also been studied using an electrochemically gated transistor,[11,20] showing that the electron mobility in these films shows a strong dependence on the number of electrons per particle. In these measurements, the mobility ranged from $10^{-7}$ m$^2$ V$^{-1}$s$^{-1}$ to $10^{-5}$ m$^2$ V$^{-1}$s$^{-1}$. These values are in good agreement with photocurrent measurements performed on electrochemical

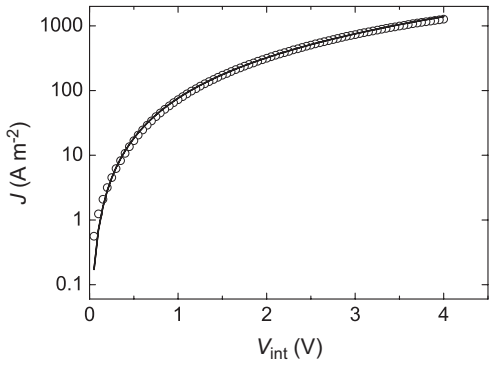


**Figure 4.** Current denstiy–voltage characteristics of electron-only diodes of MDMO-PPV/nc-ZnO (active layer thickness 115 nm). The line denotes a fit to Equation 2.

cells.[21] However, it is difficult to compare these values to the values reported here, because the volume fraction of ZnO present in the film is much lower in our case (25 vol %). Furthermore, the electron concentration in a bulk heterojunction solar cell under operating conditions[22] is several orders of magnitude lower than those reported in Roest et al.[11] and Meulenkamp.[20] On the basis of these observations, it is reasonable to expect that the mobilities found in Roest et al.,[11] Meulenkamp,[20] and Noack et al.[21] represent an upper limit to the electron mobility through the nc-ZnO phase in MDMO-PPV/nc-ZnO devices.

Recently, we have shown that the intensity dependence of the short-circuit current is determined by the ratio of electron to hole mobility,[23] leading to different values of the exponent $\alpha$ in the relation $J_{sc} \propto I^{\alpha}$.When the electron mobility is much larger (typically more than two orders of magnitude) than the hole mobility, buildup of net space charge results in $0.75 < \alpha < 1$.[24] On the other hand, if the mobilities of electrons and holes are comparable, the transport is balanced and $\alpha$ is equal to unity. The linear dependence of the short-circuit current density on light intensity (see Fig. 2, $\alpha = 1.03 \pm 0.02$), supports our findings of the electron and hole mobilities. It should be noted that Beek et al. have reported a lower value for $\alpha$, that is, 0.93.[10] However, in their investigation, the MDMO-PPV was synthesized via a different route, probably leading to a lower hole mobility, thereby leading to a lower value of $\alpha$.

### 2.3. Improvement of the Efficiency

In order to identify the factors limiting the performance of MDMO-PPV/nc-ZnO solar cells, we have applied a numerical model that includes drift and diffusion of charge carriers, the effect of space charge on electric field, and field-dependent mobilities to the data of Figure 1.[22,25] Note, that we did not consider a field-dependent generation rate of free electrons and holes, because it is not expected that this results in a significant field-dependence in the limited voltage range considered here, because of the high dielectric constant of ZnO. Using $\mu_{h0} = 5.5 \times 10^{-10}$ m$^2$ V$^{-1}$ s$^{-1}$ and $\gamma_h = 3.5 \times 10^{-4}$ (m V$^{-1}$)$^{0.5}$ for the mobility of holes, $\mu_{e0} = 3.7 \times 10^{-9}$ m$^2$ V$^{-1}$ s$^{-1}$ and

  

$\gamma_e = 0.5 \times 10^{-4}$ $(m\,V^{-1})^{0.5}$ of electrons, and a generation rate of free carriers $G = 1.26 \times 10^{27}$ $m^{-3}\,s^{-1}$, a good agreement between experimental data and numerical modeling is obtained (see Fig. 1), allowing for a detailed investigation of the factors governing the performance of these solar cells.

### *2.3.1. Comparing MDMO-PPV/PCBM with MDMO-PPV/nc-ZnO Solar Cells*

A striking feature of the MDMO-PPV/PCBM system is that the best performing solar cells contain 80 wt % PCBM (corresponding to 70 vol % PCBM, using the densities of MDMO-PPV and PCBM of Bulle–Lieuwma et al.[26]), although PCBM hardly contributes to the absorption of light. Two main reasons for the need for such high PCBM loadings can be given:[18] Surprisingly, it has been demonstrated that the hole mobility of the MDMO-PPV/PCBM blend actually increases upon addition of PCBM. At 80 wt % PCBM, the hole mobility amounts to $2.0 \times 10^{-8}$ $m^2\,V^{-1}\,s^{-1}$, which is an increase of more than two orders of magnitude compared to pristine MDMO-PPV.[27,28] Additionally, the performance of MDMO-PPV/PCBM solar cells benefits from a higher dielectric constant associated with the addition of PCBM, because this facilitates the dissociation of bound electron–hole pairs across the polymer–PCBM interface.[18]

Interestingly, the performance of MDMO-PPV/PCBM solar cells with only 25 vol % PCBM, corresponding to the composition of the best performing MDMO-PPV/nc-ZnO cells, is markedly worse with an efficiency of only 0.2 %.[18] Moreover, at that composition, the electron mobility in the PCBM phase is equal to approximately $3 \times 10^{-10}$ $m^2\,V^{-1}\,s^{-1}$ and the hole mobility equals the pristine MDMO-PPV value. Therefore, the electron mobility of the MDMO-PPV/nc-ZnO system is higher at this composition, as is the efficiency (1.6 %). The generation of free charge carriers under operating conditions in the MDMO-PPV/nc-ZnO system is more efficient ($G = 1.26 \times 10^{27}$ $m^{-3}\,s^{-1}$, for the device of Fig. 1) than in the MDMO-PPV/PCBM devices, where $G = 5 \times 10^{26}$ $m^{-3}\,s^{-1}$.[18] This is a consequence of the less efficient electron–hole pair dissociation because of the lower dielectric constant of PCBM. Our model calculations show that this changes the dissociation efficiency by more than a factor of two.

### *2.3.2. Improving the Performance of MDMO-PPV/nc-ZnO Solar Cells*

As already mentioned, the open-circuit voltage of MDMO-PPV/nc-ZnO is lower than the open-circuit voltage of MDMO-PPV/PCBM devices because of the less favorable energetic position of the conduction band of nc-ZnO. However, as we will demonstrate below, the main cause for a lower efficiency, as compared to optimized MDMO-PPV/PCBM devices, lies in the lower charge-carrier mobilities.

The concentration of nc-ZnO in these blends is limited by the film-forming properties: when more than 33 vol % of nc-ZnO is added, the film quality becomes very poor.[10] The fact that one is limited to rather low nc-ZnO content, complicates a good comparison between both systems. For example, it is at this moment unclear whether the spectacular enhancement of the hole mobility upon addition of PCBM will also be induced by nc-ZnO addition, if it were possible to maintain a good morphology. Additionally, in view of the high mobilities reported for nc-ZnO electrodes,[11,20,21] it is reasonable to assume that the electron mobility through the nc-ZnO phase would also benefit from a larger volume percentage of nc-ZnO. Additionally, Beek et al. have shown that the photoluminescence of an MDMO-PPV/nc-ZnO containing 25 vol % nc-ZnO is not completely quenched, probably because of large polymer domains in the film morphology.[10] The need for a better control over the morphology of the blend is obvious, and one option would be the use of additional ligands that improve the dispersability of the nanocrystals. However, Greenham et al. have demonstrated that the use of a ligand can seriously hamper the charge transfer from conjugated polymers to inorganic nanocrystals.[5] Huynh et al. were able to control the morphology of films consisting of CdSe nanocrystals blended with P3HT through the use of the weakly binding ligand pyridine.[29] After deposition of the blend film, the ligand could be removed by heating the sample under vacuum. Another approach is to use an electroactive ligand, which mediates the electron transfer between CdSe nanoparticles and conjugated polymers.[30,31] These results show the potential of the use of ligands for controlling the properties of polymer/inorganic nanoparticles blends.

To show that higher efficiencies can indeed be obtained once the hole mobility is improved, we have calculated the effect of improving the hole mobility up to the MDMO-PPV/PCBM (1:4 by weight) value, $2.0 \times 10^{-8}$ $m^2\,V^{-1}\,s^{-1}$, on the current density–voltage characteristics of an MDMO-PPV/nc-ZnO solar cell, see Figure 5. As expected, the efficiency of MDMO-PPV/nc-ZnO solar cells benefits from this improvement of the charge transport, and the efficiency would be enhanced by 35 %. The fact that the hole mobility is equal to the pristine MDMO-PPV value represents a limit to the efficiency that may be relieved by replacing MDMO-PPV with another, more

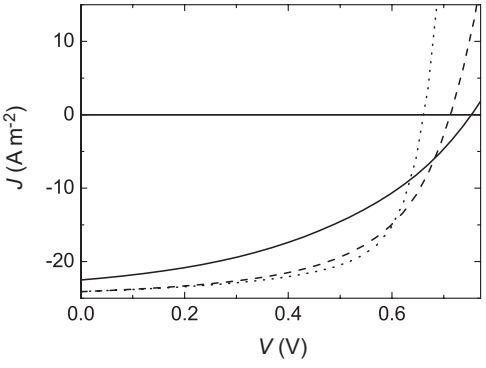


**Figure 5.** Simulated current density–voltage characteristics showing the influence of the charge-carrier mobilities. The solid line is the fit to the experimental data shown in Figure 1. The dashed line denotes the numerical result for the case when the hole mobility is increased to $2.0 \times 10^{-8}$ $m^2\,V^{-1}\,s^{-1}$, the MDMO-PPV/PCBM (1:4 by weight) value, whereas the dotted line corresponds to what would happen if the electron mobility was also increased to the standard MDMO-PPV/PCBM value of $2.0 \times 10^{-7}$ $m^2\,V^{-1}\,s^{-1}$.

ADVANCED FUNCTIONAL MATERIALS



suitable, polymer. Although bulk ZnO is a very good electron conductor, the electron mobility in the nc-ZnO phase is lower than the electron mobility of PCBM. As electron mobilities that are at least comparable to or higher than the electron mobility of PCBM have been reported,[11,23,24] it is to be expected that by fine-tuning the processing conditions, the electron mobility in the nc-ZnO phase can be improved. However, because the hole mobility is lower than the electron mobility, it is to be expected that not much is to be gained by improving the mobility of the electrons. Therefore it comes as no surprise, that also increasing the electron mobility to the PCBM value ($2.0 \times 10^{-7}$ $m^2 V^{-1} s^{-1}$) yields an only slightly higher efficiency, which is 44 % higher than the efficiency of the actual devices (see Fig. 5). The main increase in the efficiency for the system with enhanced mobilities lies in an increase in fill factor caused by the better transport of charges. As the charge-carrier mobilities are increased, the open-circuit voltage is lowered slightly[32] (see Fig. 5), because the carrier densities in the bulk of the device are lowered, because of the carriers flowing out of the device more easily. The field and carrier densities in the device, therefore, come closer to their values in the dark and hence the open-circuit voltage decreases. This implies that there is an optimum for the charge-carrier mobilities, depending on light intensity and active layer thickness. At intensities around 1 Sun, the optimal value of the mobilities is of the order of $10^{-8}$–$10^{-6}$ $m^2 V^{-1} s^{-1}$, according to our numerical model.

Ravirajan et al. have demonstrated that the hole mobility is not the limiting factor in multilayer polyer/$TiO_2$ solar cells.[33] Instead, it was found that the short-circuit current was limited by the photogeneration rate and by the quality of the interfaces, although the influence of the hole mobility on the overall device performance cannot be ruled out. This shows that each system most be evaluated on its own merits.

In a recent study, P3HT was used to replace MDMO-PPV as the electron-donor material.[34] It is well known that, depending on processing conditions, the hole mobility in the P3HT phase of P3HT/PCBM solar cells can be very high, resulting in very efficient devices.[35,36] In the case of P3HT/nc-ZnO solar cells, it was found that the efficiency increased up to 0.9 % upon thermal annealing of the devices, which is not an improvement compared to MDMO-PPV/nc-ZnO devices, despite the supposedly higher hole mobility. It is, however, unclear whether the hole mobility in the P3HT phase of the hybrid device is as high as in the P3HT/PCBM devices, because the presence of nc-ZnO may influence the crystallization of P3HT. The sublinear ($\alpha = 0.9$) intensity dependence of the short-circuit current[34] suggests that there exists at least a large difference between electron and hole mobility. Additionally, it was found that not all of the P3HT was in close proximity to ZnO, because of an unfavorable morphology, which limits the exciton-quenching process and thereby the charge-generation process. This clearly demonstrates the need for greater control over the film morphology. Another interesting approach to improve the charge generation of hybrid devices was investigated by Olson et al. who found that the efficiency of P3HT/ZnO nanofiber devices was limited by the large distance between the nanofibers.[37] By incorporating PCBM in their blends, the exciton quenching and charge generation could be significantly enhanced, leading to a power conversion in excess of 2 %.

## 3. Conclusions

We have characterized the transport of charge carriers in solar cells consisting of a blend of MDMO-PPV and nc-ZnO by selectively suppressing the injection of one of the charge carriers through the use of either high- or low-work-function electrodes. The finding of space-charge-limited currents enabled us to directly determine the mobility of electrons and holes in the blend. The hole mobility in the polymer phase of MDMO-PPV/nc-ZnO (1:2 by weight) is found to be equal to the mobility in pristine MDMO-PPV, that is, $5.5 \times 10^{-10}$ $m^2 V^{-1} s^{-1}$, whereas the electron mobility amounts to $2.8 \times 10^{-9}$ $m^2 V^{-1} s^{-1}$. The observation of a less than one order of magnitude difference between electron and hole mobility is in accordance with the linear dependence of $J_{sc}$ on incident-light intensity. The finding that the hole mobility is not to affected by the presence of nc-ZnO, in contrast to MDMO-PPV/PCBM solar cells where the hole mobility increases by more than two orders of magnitude upon addition of 70 vol % PCBM, is one of the main reasons for the lower efficiency of the MDMO-PPV/nc-ZnO system. By replacing the MDMO-PPV by a polymer with a higher hole mobility, while maintaining a favorable morphology, and by further optimizing the processing of nc-ZnO, it should be possible to reach significantly higher efficiencies.

## 4. Experimental

The materials used were MDMO-PPV synthesized by using the sulfinyl route (molecular weight $M_w = 300$ kg mol$^{-1}$, polydispersity index 2.7), nc-ZnO synthesized by using the procedure of Pacholski et al. [13], and PEDOT:PSS from H. C. Starck GmbH. The ZnO particles were dispersed in a mixture of methanol and chlorobenzene without the aid of additional surfactants or ligands.

For photovoltaic device preparation, cleaned ITO-covered glass substrates, with an active area ranging from 0.1 to 1.0 $cm^2$, were covered with a 60 nm thick layer of PEDOT:PSS by spin-coating in ambient conditions. The substrates were subsequently dried in an oven at 140 °C for 10 min. The active layer, consisting of MDMO-PPV and nc-ZnO, was spin-coated from a mixture of methanol and chlorobenzene (1:9 by volume) under a N atmosphere. A 1 nm thick layer of LiF and a 100 nm thick Al layer were deposited by thermal evaporation under vacuum ($< 2 \times 10^{-6}$ mbar; 1 mbar = 100 Pa). Current–voltage characteristics were recorded with a computer-controlled Keithley 2400 source meter under a N atmosphere. Film thicknesses were measured with a Dektak 6M stylus profiler (Veeco). A 50 W white-light halogen lamp was used to illuminate the devices, whereas the UV part of the spectrum was cut with a GG 435 nm filer. The resulting intensity amounts to 720 W $m^{-2}$.

Hole-only devices were obtained by spin-casting the active layer directly on ITO, while the LiF/Al cathode was replaced by a thermally evaporated Au electrode of 80 nm thickness. In order to construct electron-only diodes, a 1 nm Cr layer was thermally evaporated on cleaned glass substrates, followed by 50 nm of Ag and 10 nm of Sm and the active layer. As a top electrode, 10 nm of Sm topped with 80 nm of Al was employed.

Received: April 24, 2006
Revised: August 21, 2006
Published online: March 28, 2007

  

[1] S. Barth, H. Bässler, *Phys. Rev. Lett.* **1997**, *79*, 4445.
[2] N. S. Sariciftci, L. Smilowitz, A. J. Heeger, F. Wudl, *Science* **1992**, *258*, 1474.
[3] J. J. M. Halls, C. A. Walsh, N. C. Greenham, E. A. Marseglia, R. H. Friend, S. C. Moratti, A. B. Holmes, *Nature* **1995**, *376*, 498.
[4] G. Yu, J. Gao, J. C. Hummelen, F. Wudl, A. J. Heeger, *Science* **1995**, *270*, 1789.
[5] N. C. Greenham, X. Peng, A. P. Alivisatos, *Phys. Rev. B: Condens. Matter Mater. Phys.* **1996**, *54*, 17 628.
[6] A. C. Arango, S. A. Carter, P. J. Brock, *Appl. Phys. Lett.* **1999**, *74*, 1698.
[7] C. Y. Kwong, A. B. Djurišic, P. C. Chui, K. W. Cheng, W. K. Chan, *Chem. Phys. Lett.* **2004**, *384*, 372.
[8] K. M. Coakley, Y. Liu, M. D. McGehee, K. L. Frindell, G. D. Stucky, *Adv. Funct. Mater.* **2003**, *13*, 301.
[9] P. A. van Hal, M. M. Wienk, J. M. Kroon, W. J. H. Verhees, L. H. Slooff, W. J. H. van Gennip, P. Jonkheijm, R. A. J. Janssen, *Adv. Mater.* **2003**, *15*, 118.
[10] W. J. E. Beek, M. M. Wienk, R. A. J. Janssen, *Adv. Mater.* **2004**, *16*, 1009.
[11] A. L. Roest, J. J. Kelly, D. Vanmaekelbergh, E. A. Meulenkamp, *Phys. Rev. Lett.* **2002**, *89*, 36 801.
[12] S. E. Shaheen, C. J. Brabec, N. S. Sariciftci, F. Padinger, T. Fromherz, J. C. Hummelen, *Appl. Phys. Lett.* **2001**, *78*, 841.
[13] C. Pacholski, A. Kornowski, H. Weller, *Angew. Chem. Int. Ed.* **2002**, *41*, 1188.
[14] W. J. E. Beek, M. M. Wienk, M. Kemerink, X. Yang, R. A. J. Janssen, *J. Phys. Chem. B* **2005**, *109*, 9505.
[15] V. Dyakonov, *Phyica E* **2002**, *14*, 53.
[16] Z. Hu, G. Oskam, P. C. Searson, *J. Colloid Interface Sci.* **2003**, *263*, 454.
[17] P. N. Murgatroyd, *J. Phys. D: Appl. Phys.* **1970**, *3*, 151.
[18] V. D. Mihailetchi, L. J. A. Koster, P. W. M. Blom, C. Melzer, B. de Boer, J. K. J. van Duren, R. A. J. Janssen, *Adv. Funct. Mater.* **2005**, *15*, 795.
[19] P. W. M. Blom, M. J. M. de Jong, J. J. M. Vleggaar, *Appl. Phys. Lett.* **1996**, *68*, 3308.
[20] E. A. Meulenkamp, *J. Phys. Chem. B* **1999**, *103*, 7831.
[21] V. Noack, H. Weller, A. Eychmüller, *J. Phys. Chem. B* **2002**, *106*, 8514.
[22] L. J. A. Koster, E. C. P. Smits, V. D. Mihailetchi, P. W. M. Blom, *Phys. Rev. B: Condens. Matter Mater. Phys.* **2005**, *72*, 085 205.
[23] L. J. A. Koster, V. D. Mihailetchi, P. W. M. Blom, *Appl. Phys. Lett.* **2005**, *87*, 203 502.
[24] V. D. Mihailetchi, J. Wildeman, P. W. M. Blom, *Phys. Rev. Lett.* **2005**, *94*, 126 602.
[25] L. J. A. Koster, V. D. Mihailetchi, P. W. M. Blom, *Appl. Phys. Lett.* **2006**, *88*, 052 104.
[26] C. W. T. Bulle–Lieuwma, W. J. H. van Gennip, J. K. J. van Duren, P. Jonkheijm, R. A. J. Janssen, J. W. Niemantsverdriet, *Appl. Surf. Sci.* **2003**, *203–204*, 547.
[27] C. Melzer, E. Koop, V. D. Mihailetchi, P. W. M. Blom, *Adv. Funct. Mater.* **2004**, *14*, 865.
[28] S. M. Tuladhar, D. Poplavskyy, S. A. Choulis, J. R. Durrant, D. D. C. Bradley, J. Nelson, *Adv. Funct. Mater.* **2005**, *15*, 1171.
[29] W. U. Huynh, J. J. Dittmer, W. C. Libby, G. L. Whiting, A. P. Alivisatos, *Adv. Funct. Mater.* **2003**, *13*, 73.
[30] D. J. Milliron, A. P. Alivisatos, C. Pitois, C. Edder, J. M. J. Fréchet, *Adv. Mater.* **2003**, *15*, 58.
[31] J. Locklin, D. Patton, S. Deng, A. Baba, M. Millan, R. C. Advinculla, *Chem. Mater.* **2004**, *16*, 5187.
[32] L. J. A. Koster, V. D. Mihailetchi, R. Ramaker, P. W. M. Blom, *Appl. Phys. Lett.* **2005**, *86*, 123 509.
[33] P. Ravirajan, S. A. Haque, J. R. Durrant, D. D. C. Bradley, J. Nelson, *Adv. Funct. Mater.* **2005**, *15*, 609.
[34] W. J. E. Beek, M. M. Wienk, R. A. J. Janssen, *Adv. Funct. Mater.* **2006**, *16*, 1112.
[35] F. Padinger, R. S. Rittberger, N. S. Sariciftci, *Adv. Funct. Mater.* **2003**, *13*, 85.
[36] V. D. Mihailetchi, H. Xie, B. de Boer, L. J. A. Koster, P. W. M. Blom, *Adv. Funct. Mater.* **2006**, *16*, 599.
[37] D. C. Olson, J. Piris, R. T. Collins, S. E. Shaheen, D. S. Ginley, *Thin Solid Films* **2006**, *496*, 26.